

High-displacement electret-based energy harvesting system for powering leadless pacemakers from heartbeats

BILEL MAAMER¹  , NESRINE JAZIRI^{1,2} , MOHAMED HADJ SAID³ , FARES TOUNSI¹ 

¹*Systems Integration and Emerging Energies (SIE),
École nationale d'ingénieurs de Sfax, Université de Sfax
3038 Sfax, Tunisia*

²*Electronics Technology Group, Institute of Micro and Nanotechnologies MacroNano
Technische Universität Ilmenau, Gustav-Kirchhoff-Straße 1 Ilmenau 98693, Germany*

³*Center for Research in Microelectronics and Nanotechnology (CRMN)
Sousse 4050, Tunisia*

e-mail:  bilel.maamer@fsm.u-monastir.tn, fares.tounsi@isimf.rnu.tn

(Received: 18.01.2022, revised: 14.11.2022)

Abstract: In vivo biomedical devices are one of the most studied applications for vibrational energy harvesting. In this paper, we investigated a novel high-displacement device for harvesting heartbeats to power leadless implantable pacemakers. Due to the location peculiarities, certain constraints must be respected for the design of such devices. Indeed, the total dimension of the system must not exceed 5.9 mm to be usable within the leadless pacemakers and it must be able to generate accelerations lower than 0.25 m/s^2 at frequencies of less than 50 Hz. The proposed design is an electrostatic system based on a square electret of dimension 4.5 mm. It is based on the Quasi-Concertina structure, which has a very low resonant frequency of 26.02 Hz and a low stiffness of 0.492 N/m, allowing it to be very useful in such an application. Using a Teflon electret charged at 1000 V, the device was able to generate an average power of $10.06 \mu\text{W}$ at a vibration rate of 0.25 m/s^2 at the resonant frequency.

Key words: electret-based system, electrostatic harvester, energy harvesting, heartbeats vibration

1. Introduction

Cardiac pacemakers are biomedical devices that replace the natural sinoatrial (SA) node, responsible for the cardiac cycle, in the event of failure. Conventional pacemakers, used for over 50 years, consist of a pectoral pulse generator connected to one or more transvenous leads [1].



© 2023. The Author(s). This is an open-access article distributed under the terms of the Creative Commons Attribution-NonCommercial-NoDerivatives License (CC BY-NC-ND 4.0, <https://creativecommons.org/licenses/by-nc-nd/4.0/>), which permits use, distribution, and reproduction in any medium, provided that the Article is properly cited, the use is non-commercial, and no modifications or adaptations are made.

Those devices have several limitations, principally related to some local complications due to the subcutaneous pocket [1]. A possible solution to this is the leadless cardiac pacemaker (LCP). The latter is a cardiac implant that integrates the pulse generator, the lead, and the energy source into a single capsule that can be implanted into the right ventricle of the heart. The main drawback of the LCP is its limited lifespan, which is limited by the used energy storage [2]. Indeed, despite the significant advances in battery technology [3], their life expectancy is still limited, in particular because of the dimensional constraint of the capsule. To remedy this problem, researchers have been working on different potential solutions such as contactless power transfer [4], body heat energy harvesting [5], and vibration energy harvesting (VEH) [6–9], which consists of converting heartbeats into electrical energy. The main challenges in realizing such a system are the harvesting of low-frequency vibrations [10, 11] and the dimensional constraints due to the shape of the ventricles, which restrict the form of the LCP to a cylinder. This cylinder must not only contain the embedded energy harvester, which must generate power in the range of 5–10 μW [12], but also the required electrical interfaces [13]. Most harvesting systems dedicated to pacemakers are piezoelectric systems [12, 14–16] or electrostatic systems [17, 18]. Colins *et al.* [19] proposed a piezoelectric system consisting of a mass-loaded clamped-free beam using almost the entire length of the capsule, which allows reaching low frequencies. In order to improve efficiency, the beam was designed in a bimorph cantilever configuration. The beam's dimensions were $40 \times 5 \times 0.38 \text{ mm}^3$, occupying 70% of the total volume of the capsule. The average power generated was in the range of 5–12 μW with a load of 100 k Ω for vibrations simulating real heartbeats. The system proposed by Ansari *et al.* [15] is a fan-folded structure composed of 3 bimorph piezoelectric beams of dimension $20 \times 5 \times 0.19 \text{ mm}^3$ folded on top of each other. The system generated a power of 16 μW for an 80 k Ω load. Both systems generated sufficient power, however, both had to use a relatively high tip mass $> 18 \text{ g}$. Vystovsky *et al.* [17] proposed an electrostatic harvester weighing $\sim 0.5 \text{ g}$ within an overall volume $< 0.3 \text{ cm}^3$. It consists of multimodal-shaped springs in a variable capacitor with gap overlap geometry. The capacitance varied from 13 to 109 pF, generating an average power of 2.5 μW . The major drawback here is that electrostatic systems need an initial charge. To overcome this problem, the authors used a self-biased interface circuit which uses a harvested amount of energy to recharge the bias capacitance [20]. On the other hand, it is possible to overcome this limit by the use of electrets [18, 21]. In this paper, we propose a novel structure for an electret-based electrostatic energy harvester. The system was designed taking into consideration the size and energy constraints necessary for pacemakers. The rest of the paper is organized as follows: In Section 2, we will discuss the limitations and requirements of the pacemaker that have to be studied for the harvester design. We will investigate the proposed system in Section 3. In Section 4, we will discuss the results, and Section 5 concludes the paper.

2. VEH for pacemakers

2.1. Pacemakers characteristics

Currently, two types of LCPs are available in the market. The first, introduced by St. Jude Medical Group in 2012, is the NanostimTM. The second, introduced by Medtronic in 2013, is the Micra Transcatheter Pacing System (TPS) [22]. It is the only LCP approved for use in the United

States by the Food and Drug Administration (FDA) as of April 2016 [23]. Regarding the fixation mechanism, the Micra uses nitinol tines to affix to the myocardium, while the Nanostim uses an active fixation screw in the helix. Both systems are self-contained and incorporate all necessary components into a single capsule. The Micra integrates a 3-axis accelerometer and a conventional radiofrequency communication system. A battery with a capacity 120 mAh allows the device to operate autonomously for ~4.7 years [22]. On the other hand, The Nanostim capsule incorporates a temperature sensor and uses a conductive communication of ECG electrodes. The battery used for this capsule has a capacity of 248 mAh allowing a longer lifespan of ~9.8 years. Unfortunately, the latter has recently been the subject of two major recalls: one due to premature battery failure and the second due to spontaneous detachment of the docking button (a feature designed to allow retrieval of the Nanostim™) [22]. The features of interest to us are summarized in Table 1.

Table 1. Summary of the LCP general characteristics

Characteristics	Micra™	Nanostim™
Length (mm)	25.9	42
Diameter (mm)	6.7	5.99
Weight (g)	2	2
Sensor	Accelerometer	Temperature
Battery capacity (mAh)	120	248
Longevity* (year)	4.7	9.8

*Battery longevity based on the ISO14708 to report battery longevity: (2.5 V@0.4 ms), 600 Ω and fixed pacing at 60 beats/min.

2.2. Dimensional design constraints

A 3D general view of a self-sustainable LCP capsule is shown in Fig. 1. As shown in the previous sections, the LCPs have different sizes, and therefore their dimension constraints differ for the design of a proper harvesting system. For the Micra™, the system must be integrable into a capsule of length 25.9 mm and diameter of 6.7 mm while for the Nanostim™ the length limit is 42 mm and diameter 5.99 mm. Therefore, constraints over the structure's dimensions and allowed

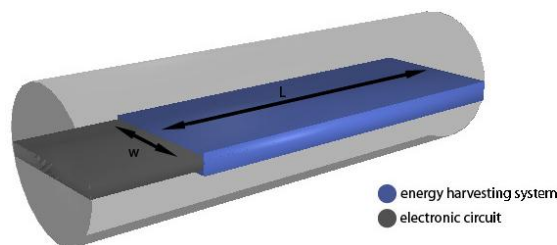


Fig. 1. Self-contained pacemaker: 3D view of the capsule

displacement must be taken into consideration. In fact, the length of the VEH system L , must be below the length of the capsule, and its width W inferior to the diameter of the capsule.

2.3. Aimed frequencies

The study of Kanai *et al.* [24] shows that the cardiac excitations act as an impulse, that is, they have a wide spectrum frequency that ranges from 1 Hz (normal heartbeat rate), where the highest acceleration of 15 m/s^2 is obtained, up to approximately 50 Hz with accelerations varying between 0.1 and 0.25 m/s^2 [25]. In order to maximize the generated power two approaches can be considered; the first is to design a broadband EH system [17]. A second possible approach is to design a resonant system which resonance frequency matches a high acceleration harmonic. In fact, the heartbeat spectrum presents harmonic with different accelerations [15]. Therefore, some resonant EH systems aims for harmonics with high accelerations such as at 15 Hz [19] and 39 Hz [25]. One of the highest accelerations are localized around 27 Hz, which will be the targeted frequency in this work.

3. Proposed system

3.1. Working principle

The principle of the proposed system, illustrated in Fig. 2(a), is an electrostatic harvester. It is composed of a variable capacitor consisting of a moving electrode stuck to the seismic mass of a vibrating structure, suspended above a fixed electrode. To cope with the problem of the initial polarization, an electret of thickness t_h and relative permittivity ϵ_r , is charged to a surface voltage of V_s and added on the fixed electrode's top. The system can be assimilated to a voltage source in series with two capacitors as shown in Fig. 2(b). When the suspended mass vibrates under the effect of an external excitation, the distance $d(t)$ between the top electrode and the electret layer varies, causing the variation of the total capacity of the system $c_t(t)$ given by:

$$c_t(t) = \frac{\epsilon_0 A}{\left[d(t) + \left(\frac{t_h}{\epsilon_r} \right) \right]}, \tag{1}$$

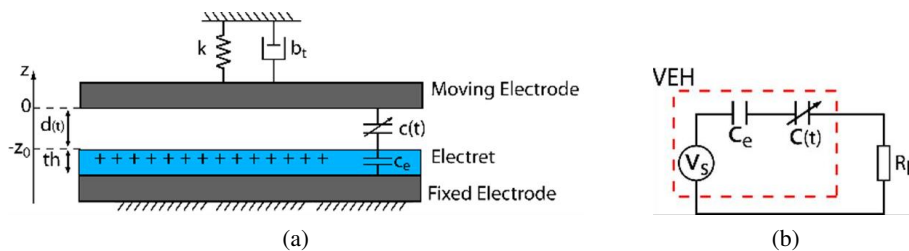


Fig. 2. Electrostatic harvester: (a) principle design; (b) electrical equivalent circuit

where A is the area of the electrodes and ϵ_0 is the vacuum permittivity. When a load resistance R_L is connected to the system, a current, denoted I , can be generated given by:

$$I = \frac{dQ}{dt} = \frac{V_s}{R_L} - \frac{Q}{R_L c_t(t)}, \quad (2)$$

where Q is the charge on the electrodes.

Assuming that the structure is subject to an external vibration $y(t)$, the moving electrodes vibrates according to:

$$m\ddot{z} = F_{\text{elec}} - (m\ddot{y} + b_t\dot{z} + kz), \quad (3)$$

where: m and k are the mass and the stiffness of the structure, respectively, $z(t)$ is the position of the moving electrode, b_t is the total damping of the system and F_{elec} is the electrostatic force between the electrodes given by:

$$F_{\text{elec}} = \frac{V_s Q(t)}{2 \left(d(t) + \left(\frac{th}{\epsilon_r} \right) \right)}, \quad (4)$$

where the distance $d(t)$ is given by:

$$d(t) = z_0 + z(t). \quad (5)$$

Hence, the instantaneous output power P will be given then by:

$$P = 0.5 F_{\text{elec}} \dot{z}. \quad (6)$$

3.2. Mechanical structure analysis

The vibrating structure is based on the Quasi-Concertina (QC) structure [26], shown in Fig. 3(a). It is designed to hold a suspended seismic mass of length l_m and thickness h_m with a set of n_b parallel beams on each side to ensure a large deflection, as shown in Fig. 3(b). The QC-structure is made of SiO_2 (with 70 GPa as Young's modulus and 2.65 g/cm^3 as density) while the proof mass is formed by silicon with a density of 2.33 g/cm^3 . Starting from the anchor, every two successive beams are identical and interconnected with joints located in the corner, forming a pair of beams. Consequently, we have $n_b/2$ pairs of beams. Then the pairs are interconnected with joints in the middle, as shown. Beams' width and space between, denoted w_b , is chosen to be equal to the thickness denoted h_b . The total oscillating structure, consisting of the seismic mass and the beams, has a square shape of dimension L_{QC} . The integration of the device in an LCP capsule is schematized in Fig. 3(c).

The QC structure can be assimilated as four similar springs k_{set} in a parallel configuration holding the seismic mass, as shown in Fig. 4(a). Each spring is formed by set of n_b beams. To simplify our model, we consider only one beam set. As a result, a quarter of the originally applied force is required to achieve the same deformation. A further simplification can be made by considering each set as $n_b/2$ springs in series, as illustrated in Fig. 4(b), where each spring $k_{p,i}$ is caused by a pair of beams. Considering i the position of a pair of beams when counting from the anchor ($1 \leq i \leq n/2$), the length $l_{b,i}$ of the two beams of the pair is given by:

$$l_{b,i} = L_{QC} - 8wi. \quad (7)$$

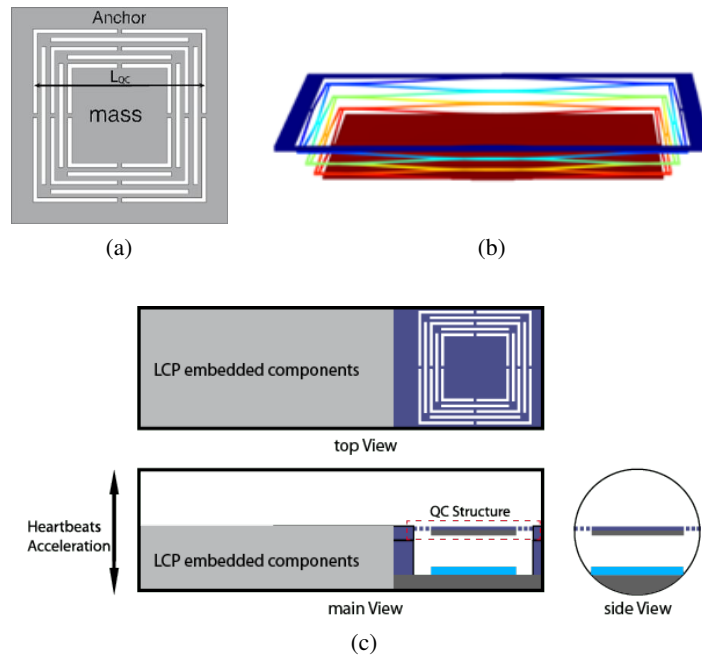


Fig. 3. QC structure: (a) top view; (b) out-of-plane deflection; (c) schematic view of the device with the VEH

Then, each pair can be modeled as four similar fixed-guided beams of length $l_{b,i}/2$ and spring constant $k_{b,i}$, as shown in the configuration in Fig. 4(c). Using Bernoulli-Euler beam theory, the equation of $k_{b,i}$ is given by:

$$k_{b,i} = \frac{8Ewh^3}{l_{b,i}^3}, \tag{8}$$

where E is the Young's modulus. A simple demonstration proves that $k_{b,i}$ is equal to $k_{p,i}$. Therefore, the spring constant of a set k_{set} is given by:

$$\frac{1}{k_{set}} = \sum_{i=1}^{n/2} \frac{1}{k_{b,i}}. \tag{9}$$

In addition, the total spring constant of the system is obtained by multiplying k_{set} by 4 for the other sides.

When the structure is subjected to a force F , each set and each pair of beams bears a quarter of this force. Consequently, the structure is deformed, and the displacement z of the seismic mass caused by this force is given by:

$$z = \frac{1}{4} \sum_{i=1}^{n/2} \frac{F}{k_{b,i}}. \tag{10}$$

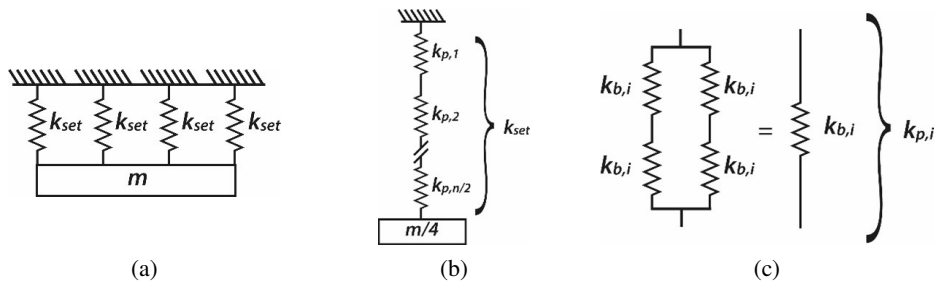


Fig. 4. QC modeling: (a) springs of sets in parallel configuration; (b) springs of pairs; (c) springs in a single pair [27]

Table 2 summarizes the characteristics of the VEH, and Fig. 3(c) the schematic view of the LCP capsule with the integrated VEH, respectively. With these dimensions, the obtained stiffness of the structure, k_{set} , was about 0.4922 N/m with a resonance frequency equal to 26.02 Hz.

Table 2. Characteristics of the proposed system

Number of beams, n	6
Length of the structure, L_{QC}	4.5 mm
Width of beams, w	20 μm
Thickness of beams, h_b	10 μm
Length of the membrane (electrode), l_m	3.98 mm
Thickness of proof mass, h_m	500 μm
Initial gap, z_0	100 μm
Electret material	Teflon
Electret thickness, h_e	100 μm
Electret charge, V_s	1000 V

4. Simulation results

When an excitation of 0.25 m/s^2 is applied at a frequency of 26 Hz, the displacement $z(t)$ and the total capacity $ct(t)$ variation of the system are shown in Fig. 5(a). We can observe that the structure's peak-to-peak displacement is about $\sim 200 \mu\text{m}$, allowing a capacitance variation from 0.6 pF to 2.5 pF. Considering that the voltage is kept constant with the charged electret [10], the capacitance variation results in a charge variation, generating a current as explicated in Eq. (2). Therefore, the generated current is presented in Fig. 5(b). It can be seen that when the capacitance increases, the generated current rises up to 0.2 μA , while when it decreases, a higher negative

value of $0.25 \mu\text{A}$ is obtained. This difference could be caused by the electrostatic force, which is stronger when the electrodes are brought closer together (high capacitance), requiring a higher force to pull them apart (decreasing the capacitance). When connected to a load resistance of $500 \text{ M}\Omega$, the power generated is illustrated in Fig. 5(c). Two peak powers of 20 and $27 \mu\text{W}$ can be seen to be obtained at the increasing and decreasing slopes of the capacitance. The average generated power is $10.6 \mu\text{W}$ which would be sufficient for powering pacemakers [12].

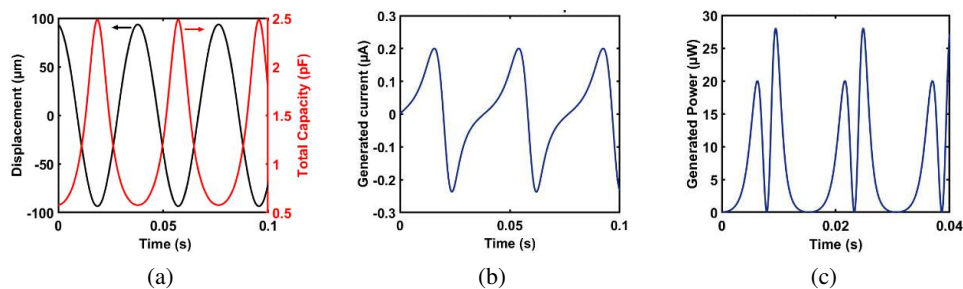


Fig. 5. (a) displacement and total capacity of the system under vibration of 0.25 m/s^2 @26 Hz; (b) generated current; (c) generated power with a load of $500 \text{ M}\Omega$

5. Conclusion

Vibration energy harvesters (VEH) are a potential solution for powering leadless cardiac pacemakers (LCP). However, certain constraints must be respected for the device to be suitable for the application. We have presented in this paper a brief review of the challenges of HEV design for LCP. First, the characteristics of available LCPs are presented. The dimension of the harvester must not exceed 5.9 mm to fit into an LCP enclosure. With this, it should be able to generate power under accelerations of 0.25 m/s^2 at frequencies below 50 Hz . By knowing this, we investigated an electret-based gap-closing electrostatic system. The system is based on a quasi-concertina structure that allows a high out-of-plane displacement. The system's length is 4.5 mm , allowing it to fit into the LCP. With a resonance frequency of 26.06 Hz and a low stiffness of 0.492 N/m , the system was able to vibrate under an acceleration of 0.25 m/s^2 at the resonant frequency, achieving a displacement of $200 \mu\text{m}$. The total capacity of the system has been multiplied by 4, allowing it to generate an average power of $10.06 \mu\text{W}$.

References

- [1] Miller M.A., Neuzil P., Dukkupati S.R., Reddy V.Y., *Leadless Cardiac Pacemakers: Back to the Future*, Journal of the American College of Cardiology, vol. 66, no. 10, pp. 1179–1189 (2015), DOI: [10.1016/j.jacc.2015.06.1081](https://doi.org/10.1016/j.jacc.2015.06.1081).
- [2] Hallmann M., Wenge C., Komarnicki P., Balischewski S., *Methods for lithium-based battery energy storage SOC estimation. Part I: Overview*, Archives of Electrical Engineering, vol. 71, no. 1, pp. 139–157 (2022), DOI: [10.24425/ae.2022.140202](https://doi.org/10.24425/ae.2022.140202).

- [3] Riaz A., Sarker M.R., Saad M.H.M., Mohamed R., *Review on comparison of different energy storage technologies used in micro-energy harvesting, WSNs, low-cost microelectronic devices: challenges and recommendations*, *Sensors*, vol. 21, no. 15, p. 5041 (2021), DOI: [10.3390/s21155041](https://doi.org/10.3390/s21155041).
- [4] Ghosh P.C., Sadhu P.K., Ghosh A., Pal N., *A new circuit topology using Z-source resonant inverter for high power contactless power transfer applications*, *Archives of Electrical Engineering*, vol. 66, no. 4 (2017), DOI: [10.1515/ae-2017-0064](https://doi.org/10.1515/ae-2017-0064).
- [5] Bose S., Shen B., Johnston M.L., *A batteryless motion-adaptive heartbeat detection system-on-chip powered by human body heat*, *IEEE Journal of Solid-State Circuits*, vol. 55, no. 11, pp. 2902–2913 (2020), DOI: [10.1109/JSSC.2020.3013789](https://doi.org/10.1109/JSSC.2020.3013789).
- [6] Maamer B., Jaziri N., Kaziz S., Tounsi F., *Towards Autonomous Node Sensors: Green Versus RF Energy Harvesting*, in *IEEE International Conference on Design and Test of Integrated Micro and Nano-Systems (DTS)*, pp. 1–5 (2021), DOI: [10.1109/DTS52014.2021.9498247](https://doi.org/10.1109/DTS52014.2021.9498247).
- [7] Liu L., Guo X., Liu W., Lee C., *Recent progress in the energy harvesting technology—from self-powered sensors to self-sustained IoT, and new applications*, *Nanomaterials*, vol. 11, no. 11, p. 2975 (2021), DOI: [10.3390/nano11112975](https://doi.org/10.3390/nano11112975).
- [8] Garus S., Błachowski B., Sochacki W., Jaskot A., Kwiaton P., Ostrowski M., Šofer M., Kapitaniak T., *Mechanical vibrations: recent trends and engineering applications*, *Bulletin of the Polish Academy of Sciences: Technical Sciences*, vol. 70, no. 1, p. e140351 (2022), DOI: [10.24425/bpasts.2022.140351](https://doi.org/10.24425/bpasts.2022.140351).
- [9] Blad T., *Micro Energy Harvesting from Low-Frequency Vibrations: Towards Powering Pacemakers with Heartbeats*, Ph.D. dissertation, Delft University of Technology (2021).
- [10] Maamer B., Boughamoura A., El-Bab A.M.F., Francis L.A., Tounsi F., *A review on design improvements and techniques for mechanical energy harvesting using piezoelectric and electromagnetic schemes*, *Energy Conversion and Management*, vol. 199, p. 111973 (2019), DOI: [10.1016/j.enconman.2019.111973](https://doi.org/10.1016/j.enconman.2019.111973).
- [11] Atmeh M., Ibrahim A., *Modeling of Piezoelectric Vibration Energy Harvesting from Low-Frequency Using Frequency Up-Conversion*, *Smart Materials, Adaptive Structures and Intelligent Systems*, vol. 85499, p. V001T04A011 (2021), DOI: [10.1115/SMASIS2021-68360](https://doi.org/10.1115/SMASIS2021-68360).
- [12] Jay S., Caballero M., Quinn W., Barrett J., Hill M., *Characterization of piezoelectric device for implanted pacemaker energy harvesting*, *Journal of Physics: Conference Series*, vol. 757, no. 1, p. 012038 (2016), DOI: [10.1088/1742-6596/757/1/012038](https://doi.org/10.1088/1742-6596/757/1/012038).
- [13] Lombardi G., *Unified nonlinear electrical interfaces for hybrid piezoelectric-electromagnetic small-scale harvesting systems*, Ph.D. dissertation, National Institute of Applied Sciences, University of Lyon (2020).
- [14] Kumar A., Kiran R., Chauhan V.S., Kumar R., Vaish R., *Piezoelectric energy harvester for pacemaker application: a comparative study*, *Materials Research Express*, vol. 5, no. 7, p. 075701 (2018), DOI: [10.1088/2053-1591/aab456](https://doi.org/10.1088/2053-1591/aab456).
- [15] Ansari M., Karami M.A., *Experimental investigation of fan-folded piezoelectric energy harvesters for powering pacemakers*, *Smart Materials and Structures*, vol. 26, no. 6, p. 065001 (2017), DOI: [10.1088/1361-665X/aa6cfd](https://doi.org/10.1088/1361-665X/aa6cfd).
- [16] Jackson N., Olszewski O.Z., O’Murchu C., Mathewson A., *Shock-induced aluminum nitride based MEMS energy harvester to power a leadless pacemaker*, *Sensors and Actuators A: Physical*, vol. 264, pp. 212–218 (2017), DOI: [10.1016/j.sna.2017.08.005](https://doi.org/10.1016/j.sna.2017.08.005).
- [17] Vysotskyi B., Parrain F., Le Roux X., Lefeuvre E., Gaucher P., Aubry D., *Electrostatic vibration energy harvester using multimodal-shaped springs for pacemaker application*, in *Symposium on Design, Test, Integration and Packaging of MEMS and MOEMS (DTIP)*, pp. 1–6 (2018), DOI: [10.1109/DTIP.2018.8394216](https://doi.org/10.1109/DTIP.2018.8394216).

- [18] Ahmed S., Kakkar V., *An electret-based angular electrostatic energy harvester for battery-less cardiac and neural implants*, IEEE Access, vol. 5, pp. 19631–19643 (2017), DOI: [10.1109/ACCESS.2017.2739205](https://doi.org/10.1109/ACCESS.2017.2739205).
- [19] Colin M., Basrou S., Rufer L., *Design, fabrication and characterization of a very low frequency piezoelectric energy harvester designed for heartbeat vibration scavenging*, Smart Sensors, Actuators, and MEMS VI, vol. 8763, p. 87631P (2013), DOI: [10.1117/12.2017439](https://doi.org/10.1117/12.2017439).
- [20] Lefeuvre E., Risquez S., Wei J., Woytasik M., Parrain F., *Self-biased inductor-less interface circuit for electret-free electrostatic energy harvesters*, Journal of Physics: Conference Series, vol. 557, no. 1, p. 012052 (2014), DOI: [10.1088/1742-6596/557/1/012052](https://doi.org/10.1088/1742-6596/557/1/012052).
- [21] Bi M., Wu Z., Wang S., Cao Z., Cheng Y., Ma X., Ye X., *Optimization of structural parameters for rotary freestanding-electret generators and wind energy harvesting*, Nano Energy, vol. 75, p. 104968 (2020), DOI: [10.1016/j.nanoen.2020.104968](https://doi.org/10.1016/j.nanoen.2020.104968).
- [22] Bhatia N., El-Chami M., *Leadless pacemakers: a contemporary review*, Journal of geriatric cardiology: JGC, vol. 15, no. 4, p. 249 (2018), DOI: [10.11909/j.issn.1671-5411.2018.04.002](https://doi.org/10.11909/j.issn.1671-5411.2018.04.002).
- [23] Sideris S., Archontakis S., Dilaveris P., Gatzoulis K.A., Trachanas K., Sotiropoulos I., Arsenos P., Tousoulis D., Kallikazaros I., *Leadless cardiac pacemakers: current status of a modern approach in pacing*, Hellenic Journal of Cardiology, vol. 58, no. 6, pp. 403–410 (2017), DOI: [10.1016/j.hjc.2017.05.004](https://doi.org/10.1016/j.hjc.2017.05.004).
- [24] Kanai H., Sato M., Koiwa Y., Chubachi N., *Transcutaneous measurement and spectrum analysis of heart wall vibrations*, IEEE Transactions on Ultrasonics, Ferroelectrics, and Frequency Control, vol. 43, no. 5, pp. 791–810 (1996), DOI: [10.1109/58.535480](https://doi.org/10.1109/58.535480).
- [25] Karami M.A. Inman D.J., *Linear and nonlinear energy harvesters for powering pacemakers from heart beat vibrations*, Active and Passive Smart Structures and Integrated Systems 2011, vol. 7977, p. 797703 (2011), DOI: [10.1117/12.880168](https://doi.org/10.1117/12.880168).
- [26] Grech D., *Development of a Quasi-concertina MEMS sensor for the characterisation of biopolymers*, Ph.D. dissertation, University of Southampton (2014).
- [27] Maamer B., Fath El-Bab A.M.R., Tounsi F., *Impact-Driven Frequency-Up Converter Based on High Flexibility Quasi-Concertina Spring for Vibration Energy Harvesting*, Energy Conversion and Management, vol. 274, p. 116460 (2022), DOI: [10.1016/j.enconman.2022.116460](https://doi.org/10.1016/j.enconman.2022.116460).